Local structure of A-atom in ABO_3 perovskites studies by RMC-EXAFS

Andris Anspoks[a,*], Carlo Marini[b], Takafumi Miyanaga[c], Boby Joseph[d], Alexei Kuzmin[a], Juris Purans[a], Janis Timoshenko[e], Annette Bussmann-Holder[f]

[a]*Institute of Solid State Physics, University of Latvia, Kengaraga street 8, LV-1063 Riga, Latvia*
[b]*ALBA Synchrotron Light Source, Crta. BP 1413, Km. 3.3, 08290 Cerdanyola Del Vallès, Barcelona, Spain*
[c]*Hirosaki University, Japan*
[d]*Elettra-Sincrotrone Trieste, Trieste, Italy*
[e]*Department of Materials Science and Chemical Engineering, Stony Brook University, Stony Brook, NY 11794, USA*
[f]*Max-Planck-Institute for Solid State Research, Heisenbergstr. 1, D-70569 Stuttgart, Germany*

Abstract

The ferroelectric distortions in perovskites were a subject of numerous investigations for a long time. However, some controversial results still exist, coming from the analysis of diffraction (X-ray, neutron or electron) data and X-ray absorption spectra. In this study, our goal was to revisit these classical materials using recently developed methods without imposing any predefined structural model. Local environment around A-type atom in ABO_3 perovskites ($SrTiO_3$, $BaTiO_3$, $EuTiO_3$) was studied by X-ray absorption spectroscopy (XAS) in a wide range of temperatures (20–400 K). Using reverse Monte Carlo method enhanced by evolutionary algorithm, the 3D structure was extracted from the extended X-ray absorption fine structure (EXAFS) and interpreted in terms of the radial distribution functions (RDFs). Our findings show that both diffraction and XAS data are consistent, but reflect the structure of the material from different points of view. In particular, when strong correlations in the motion of certain atoms are present, the information obtained by XAS might lead to a different from expected shape of the RDF. At the same time, the average positions of all atoms are in good agreement with those given by diffraction. This makes XAS an important technique for studying interatomic correlations and lattice dynamics.

Keywords: Extended X-ray absorption fine structure (EXAFS), X-ray absorption near edge structure (XANES), Reverse Monte Carlo, Correlation effects, Perovskites

1. Introduction

ABO_3-type perovskite materials are used in numerous technological applications such as multi-layer ceramic capacitors, transducers and actuators, catalysts, electro-optical devices, waveguides, memory cells (Cohen, 1992).

In this study, we concentrate on $BaTiO_3$, $SrTiO_3$ and $EuTiO_3$ titanates, which exhibit several low-temperature structural phase transitions (Cohen, 1992; Ravel et al., 1998; Bussmann-Holder et al., 2011; Koehler et al., 2012).

$BaTiO_3$ (BTO) has the richest phase diagram, and its structure experiences the most pronounced structural distortions. The phase transitions in $BaTiO_3$ occur on heating from polar rhombohedral to orthorhombic phase at 183 K, next to tetragonal phase at 278 K, and, finally, to paraelectric cubic phase at 393 K (Tkacz-Åmiech et al., 2003).

$SrTiO_3$ (STO) has much simpler phase diagram and very small distortions of the lattice, transforming from tetragonal to cubic phase at 105 K. At the same time, at low temperatures (<30 K), $SrTiO_3$ becomes a quantum paraelectric, because of the supression of ferroelectric ordering by quantum fluctuations (Müller and Burkard, 1979).

This makes BTO and STO a good model objects for further studies and for interpreting the structural changes that occur in ABO_3-type perovskite materials.

The third perovskite, $EuTiO_3$ (ETO), has less known phase diagram and is isostructural to $SrTiO_3$. It was considered for a long time as cubic, but a tetragonal to cubic phase transition was discovered recently at 282 K (Schiemer et al., 2016). ETO is even more complex compound, since it has also antiferromegnetic phase below T_N=5.5 K, and some anomalies were discovered around 190 K (Stuhlhofer et al., 2016).

The ABO_3 perovskites were intensively studied in the past by many methods including X-ray absorption spectroscopy (XAS). The main focus of XAS studies was on the TiO_6 octahedra responsible for ferroelectric properties of these materials. The Ti *K*-edge X-ray absorption near edge structure (XANES) contains several features, which are sensitive to the local symmetry and structural distortions (Vedrinskii et al., 1998). The XANES of A-atoms is less informative, therefore it is not surprising that the most XANES studies were concentrated on the Ti *K*-edge followed by the extended X-ray absorption fine structure (EXAFS) experiments (Ravel et al., 1998; Anspoks et al., 2014,

*Corresponding author
E-mail address: andris.anspoks@cfi.lu.lv (Andris Anspoks).

2015, 2016; Cockayne et al., 2018). However, in many EXAFS studies the absorption edge of A-atom was used to validate structure models, especially for solid solutions (Miyanaga et al., 2002; Mastelaro et al., 2015; Levin et al., 2016).

The A atom is well suited as a reference point since it forms the sublattice, which determines the unit cell of these perovskites. At the same time *ab initio* studies (Aschauer and Spaldin, 2014) show that the displacements of non-lone-pair A ion are comparable to those of Ti and play significant role in structural and ferroelectric phase transitions of ABO_3 perovskite. Therefore, we will focus on the local structure of the A atom in ABO_3 perovskites. We used recently developed combination of reverse Monte Carlo and evolutionary algorithm (Timoshenko et al., 2014) to reconstruct the structure of $SrTiO_3$, $BaTiO_3$ and $EuTiO_3$ using the Sr *K*-edge, Ba *K*-edge and Eu L_3-edge EXAFS spectra, collected in a wide temperature range covering the most interesting structural phases.

Most of the XAS studies of titanate perovskites lead to the results confronting with the data obtained from diffraction experiments and are best summarized in the classical work by Edward A Stern (Stern, 2004). Most of the discussions result in a dispute between displacive model of phase transition versus order-disorder type. Therefore, our goal was to revisit interpretation of EXAFS in these classical materials using recently developed methods of 3D structure reconstruction.

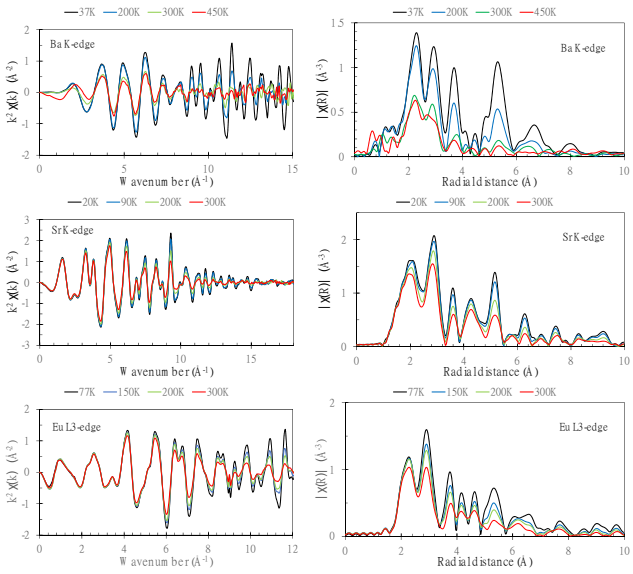

Figure 1: Temperature dependent EXAFS and Modulus of the FT-EXAFS spectra for $BaTiO_3$ (Ba *K*-edge), $SrTiO_3$ (Sr *K*-edge), $EuTiO_3$ (Eu L_3-edge).

2. Experimental

The experimental EXAFS spectra at the Ba *K*-edge of BTO were collected by Bruce Ravel and experimental details can be found in (Ravel et al., 1998).

The experimental EXAFS spectra at the Sr *K*-edge of STO were collected at the BL7C beamline of Photon Factory in KEK. The fine powder $SrTiO_3$ (99.99 %) was purchased from Soekawa Co. Ltd. The spectra were collected in transmission mode using two ionization chambers and Si(111) double-crystal monochromator.

Transmission EXAFS measurements at the Eu L_3-edge were performed in q-EXAFS mode at the CLAESS beamline (Simonelli et al., 2016) of ALBA Synchrotron (Barcelona, Spain). The intensity of the monochromatic x-ray beam, produced by a Si(111) double-crystal monochromator, was measured by two ionization chambers filled with appropriate mixtures of N_2 and Kr gases. For the temperature-dependent XAS measurements, ETO powder was diluted in an inert matrix (BN) and pressed into a pellet. The sample was inserted into a liquid-nitrogen cryostat and the temperature was varied between 77 and 377 K, controlled by a feedback loop electric heater.

The extraction of the EXAFS spectra was done using conventional methodology and Athena software (Aksenov et al., 2006; Ravel and Newville, 2005).

A pronounced temperature dependence was observed in all EXAFS spectra (Fig. 1). The strongest effect is observed in BTO, because the largest structural changes occur in this compound upon a series of the phase transitions starting from rhombohedral to orthorombic, next to tetragonal and finally to cubic phase. At the same time, the main origin of the EXAFS signal damping in STO and ETO is due to thermal disorder.

3. Reverse Monte Carlo simulations

The EXAFS spectra were analysed by reverse Monte Carlo (RMC) method based on evolutionary algorithm (EA) implemented in the EvAX code (Timoshenko et al., 2014). In this method, 3D model of material structure is obtained in a iterative process, involving random displacements of atoms with the aim to minimize the difference between the experimental and calculated EXAFS spectra. The equilibrium perovskite structure was employed as initial configuration for RMC/EA simulations with the lattice parameter and atomic positions known from diffraction experiments. We used a supercell 4×4×4 containing 640 atoms with periodic boundary conditions, and the lattice parameter and shape of the supercell were fixed during simulations.

The configuration averaged EXAFS spectra were calculated using ab-initio real-space multiple-scattering (MS) self-consistent FEFF8.5L code (Ankudinov et al., 1998). Scattering paths with the half-length up to 7.0 Å were determined for each atomic configuration and used in the calculations. The MS effects with up to seven scatterers were taken into account. For comparison of the experimental and theoretical EXAFS spectra in *k* and *R* spaces simultaneously, we relied on the Morlet wavelet transform (Timoshenko and Kuzmin, 2009). The obtained 3D structural model was used to calculate all structural parameters via statistical analysis of atomic coordinates. More technical details are given in Timoshenko et al. (2014).

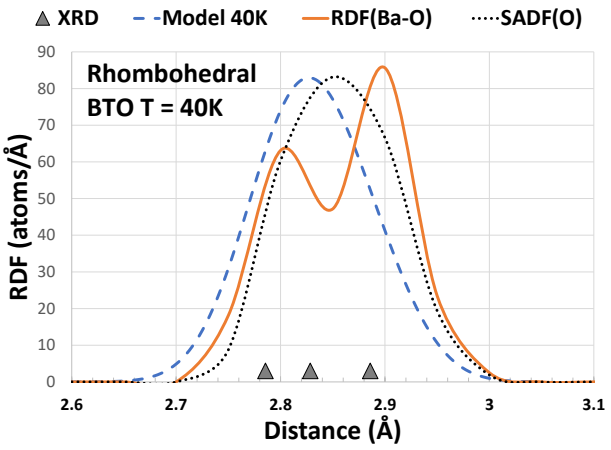

Figure 2: Model radial distribution function (RDF) for Ba–O at T=40 K compared to RDF and single atom distribution function (SADF) obtained from $BaTiO_3$ Ba K-edge EXAFS spectra using our RMC/EA-EXAFS analysis.

4. Results and discussion

The low temperature rhombohedral phase of $BaTiO_3$ was used as a starting point of our analysis as it is one phase where the most parties agree (Ravel et al., 1998; Stern, 2004) and lattice distortions (compared to cubic phase) are big and well analysed by x-ray and neutron diffraction methods. According to diffraction data (Kwei et al., 1993), it contains twelve oxygen atoms around each Ba atom, and Ba–O distances can be grouped into three groups: 3×2.786 Å, 6×2.828 Å and 3×2.886 Å. This information was used to calculate the radial distribution function (RDF) as a sum of three Gaussians (dashed line in Fig. 2). The widths of Gaussian peaks were taken as 0.044 Å(best matching experimental data and representing combination of O and Ba atomic mean squared displacements). This naive approach corresponds to the model of non-correlated atoms and harmonic interatomic potentials. Note that thus obtained RDF has rather symmetric shape with a weak shoulder towards long distances.

The atomic coordinates obtained from RMC-EXAFS simulations (Timoshenko et al., 2014; Anspoks et al., 2015; Timoshenko et al., 2016) were used to calculate two distribution functions: (i) the RDF(Ba–O) for the Ba–O distances (dotted line in Fig. 2), and (ii) the single atom distribution function (SADF) for oxygen atoms relative to the average position of the Ba atom (solid line in Fig. 2). Note that the SADF(O) does not include any correlation effects. Comparing the model RDF with the SADF(O), one can see that the two functions have quite close shapes but the SADF(O) maximum is shifted to larger distances by ~0.3 Å. At the same time, the RDF(Ba–O) has two well resolved peaks located at ~2.8 Å and ~2.9 Å and, thus, it differs significantly from both the model RDF and the SADF(O).

The difference between interatomic distances obtained by diffraction (R) and EXAFS (r) is due to the atom displacements in the direction orthogonal to the interatomic bond (Fornasini et al., 2017)

$$r = R + \langle \Delta u_\perp{}^2 \rangle / 2R, \quad (1)$$

where $\langle \Delta u_\perp{}^2 \rangle$ is the perpendicular mean-square relative displacement (MSRD). Therefore, one can expect to have slightly longer Ba–O distances from EXAFS analysis than from diffraction data, and the difference between the two gives valuable information on the perpendicular MSRD $\langle \Delta u_\perp{}^2 \rangle$. The differences in the amplitude of perpendicular motion for different atom groups may result in the change of the RDF shape.

Another factor affecting the width of the RDF is a correlation of atom motion along the interatomic direction (Rehr and Albers, 2000)

$$\sigma_{\mathrm{Ba-O}}{}^2 = \langle u_{\mathrm{Ba}}^2 \rangle + \langle u_{\mathrm{O}}^2 \rangle - 2\langle u_{\mathrm{Ba}} u_{\mathrm{O}} \rangle, \quad (2)$$

where the first two terms are the mean-square displacement (MSD) factors for Ba and O atoms, and the last term is a displacement correlation function for the pair of Ba and O atoms. Note that both of these effects (1) and (2) can change the shape of the RDF, resulting in bi-modal shape of RDF for Ba–O, as shown in Fig. 2. Similar splitting of RDF peaks is observed also in for Ba-Ti pair (Fig. 3).

Comparing RDF for all phases of BTO, we see that it is widening with the increase of temperature as amplitude of atomic vibrations increase, but the two groups of Ba–Ti distances are maintained in all phases. At the same time, the distribution of the nearest neighbors Ba–O distances for all temperatures is noticeably wider than that for Ba–Ti as second nearest neighbor, despite that a spread of the Ba–Ti distances for equilibrium positions (1×3.370 Å, 3×3.430 Å, 3×3.501 Å and 1×3.583 Å at 40 K) is comparable to that for Ba–O (3×2.786 Å, 6×2.828 Å and 3×2.886 Å at 40 K). Usually it is expected that RDF becomes wider for further coordination shells as a correlation diminishes with increasing of the distance Jonane et al. (2018). So, it is a very clear indicator that we have observed a pronounced Ba–Ti correlation in the second coordination shell of Ba. Also, recent theoretical studies about precursor effects and coexistence of order-disorder and displacive dynamics in perovskite ferroelectrics Bussmann-Holder et al. (2009) show that the correlation between nearest unit cells is maintained even at high temperatures including cubic paraelectric phase.

As TiO_6 octahedra is formed by a strong Ti–O covalent bonding (Abramov et al., 1995; Ikeda et al., 1998), so oxygen ions are more linked to Ti and it is no surprise that Ba–O movements are less correlated especially taking into account ionic bonding and twelve-fold coordination of Ba–O.

$SrTiO_3$ is another classical example. STO has cubic structure which becomes tetragonal below T_S = 105 K. Corresponding lattice distortions are small compared with BTO, so, it is a good test for small scale distortions to evaluate the sensitivity of the method.

Looking on radial distribution function for STO covering tetragonal and cubic phases, we see very similar to BTO trends. For Sr–O RDF we do not see any specific behavior as the distortions relative to cubic phase are small. Whereas Sr–Ti RDF shows two groups of atoms at 3.35 Å and 3.45 Å similar to the

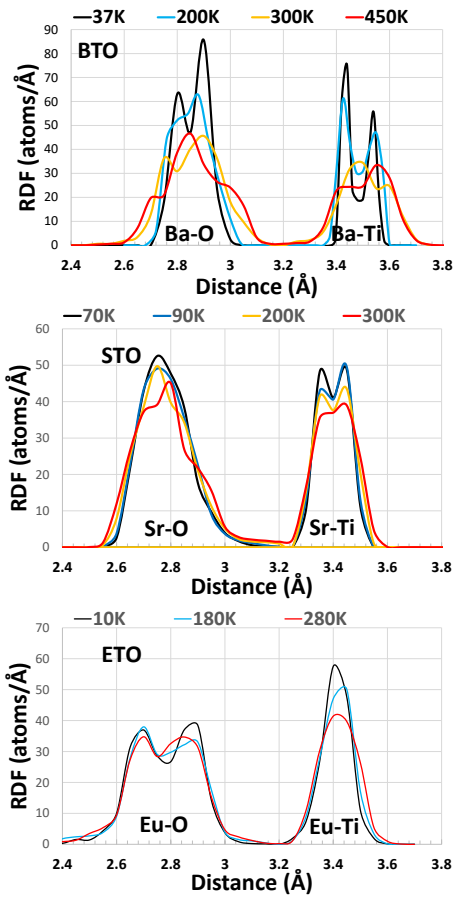

Figure 3: Radial distribution functions (RDF) for Ba–O, Ba–Ti, Sr–O, Sr–Ti, Eu–O, Eu–Ti at different temperatures obtained from $BaTiO_3$, $SrTiO_3$, $EuTiO_3$ EXAFS spectra using our RMC/EA-EXAFS analysis.

BTO, but closer to each other than in BTO. Also the shape of RDF is less changing with the temperature.

Taking into account data for STO, we now can have a fresh look on $EuTiO_3$ which is isostructural to STO, so, we expect the same RDF shape. But in reality we obtain two well separated and sustainable groups for Eu–O, and one group for Eu–Ti for the whole temperature range. The very important difference between ETO and STO is magnetic interaction which has an effect also in high temperatures far above T_N=5.5 K, for example, temperature for cubic-tatragonal phase transition can be changed by magnetic field (Guguchia et al., 2012).

5. Conclusions

By RMC/EA-EXAFS analysis we obtained original information about the local atomic structure of A ion in perovskites $BaTiO_3$, $SrTiO_3$, $EuTiO_3$ showing dynamic correlation effects of A ion with ions in the first and second coordination shell (A–O and A–Ti). These correlation effects lead to different shapes of RDF relative to the instant position of the A ion (absorber) compared to ones expected in uncorrelated model.

BTO, STO and ETO have strong Ba–Ti, Sr–Ti and Eu–Ti correlations showing that A ion plays active role in formation of ferroelectric and other ferroic phases in $ATiO_3$ perovskites.

ETO (isostructural to STO) has pronounced Eu–O correlation effects, and different Eu–Ti correlation compared to STO, caused by presence of magnetic effects.

Our observation support assumptions (Bussmann-Holder et al., 2009) that the correlations between nearest unitcells are maintained at all temperatures in all phases including cubic phase. We must note that these are dynamic correlations not static distortions. At the same time, with our analysis we confirm that the average atomic positions correspond to the data obtained from diffraction.

Acknowledgements

The measurements of Sr K-edge XAFS were performed under the approval of Proposal No. 97G042 of Photon Factory (KEK) and partially supported by the Research Grants of Hirosaki University. This work was supported by Bruce Ravel providing data for BTO. Boby Joseph acknowledges IISc Bangalore and ICTP Trieste for financial support through the award of the IISc-ICTP fellowship.

References

Abramov, Y.A., Tsirelson, V.G., Zavodnik, V.E., Ivanov, S.A., D., B.I., 1995. The chemical bond and atomic displacements in srtio$_3$ from x-ray diffraction analysis. Acta Crystallographica Section B 51, 942–951. doi:10.1107/S0108768195003752.

Aksenov, V.L., Koval'chuk, M.V., Kuz'min, A.Y., Purans, Y., Tyutyunnikov, S.I., 2006. Development of methods of EXAFS spectroscopy on synchrotron radiation beams: Review. Crystallography Rep. 51, 908–935. doi:10.1134/S1063774506060022.

Ankudinov, A.L., Ravel, B., Rehr, J.J., Conradson, S.D., 1998. Real-space multiple-scattering calculation and interpretation of x-ray-absorption near-edge structure. Phys. Rev. B 58, 7565–7576. doi:10.1103/PhysRevB.58.7565.

Anspoks, A., Bocharov, D., Purans, J., Rocca, F., Sarakovskis, A., Trepakov, V., Dejneka, A., Itoh, M., 2014. Local structure studies of (SrTiO3)-O-16 and (SrTiO3)-O-18. PHYSICA SCRIPTA 89. doi:{10.1088/0031-8949/89/04/044002}.

Anspoks, A., Timoshenko, J., Bocharov, D., Purans, J., Rocca, F., Sarakovskis, A., Trepakov, V., Dejneka, A., Itoh, M., 2015. Local Structure Studies of Ti for (SrTiO3)-O-16 and (SrTiO3)-O-18 by Advanced X-ray Absorption Spectroscopy Data Analysis. FERROELECTRICS 485, 42–52. doi:{10.1080/00150193.2015.1060102}. 12th Russia/CIS/Baltic/Japan Symposium on Ferroelectricity (RCBJSF) and 9th International Conference on Functional Materials and Nanotechnologies (FM&NT), Riga, LATVIA, SEP 29-OCT 02, 2014.

Anspoks, A., Timoshenko, J., Purans, J., Rocca, F., Trepakov, V., Dejneka, A., Itoh, M., 2016. Local dynamics and phase transition in quantum paraelectric SrTiO3 studied by Ti K-edge x-ray absorption spectroscopy 712. doi:{10.1088/1742-6596/712/1/012101}. 16th International Conference on X-ray Absorption Fine Structure (XAFS), Karlsruhe Inst Technol, Karlsruhe, GERMANY, AUG 23-28, 2015.

Aschauer, U., Spaldin, N.A., 2014. Competition and cooperation between antiferrodistortive and ferroelectric instabilities in the model perovskite srtio$_3$. Journal of Physics: Condensed Matter 26, 122203. doi:10.1088/0953-8984/26/12/122203.

Bussmann-Holder, A., Beige, H., Völkel, G., 2009. Precursor effects, broken local symmetry, and coexistence of order-disorder and displacive dynamics in perovskite ferroelectrics. Phys. Rev. B 79, 184111. doi:10.1103/PhysRevB.79.184111.

Bussmann-Holder, A., Koehler, J., Kremer, R.K., Law, J.M., 2011. Relation between structural instabilities in EuTiO3 and SrTiO3. PHYSICAL REVIEW B 83. doi:{10.1103/PhysRevB.83.212102}.

Cockayne, E., Shirley, E.L., Ravel, B., Woicik, J.C., 2018. Local atomic geometry and ti 1s near-edge spectra in pbtio$_3$ and srtio$_3$. Phys. Rev. B 98, 014111. doi:10.1103/PhysRevB.98.014111.

Cohen, R., 1992. Origin of Ferroelectricity in Perovskite Oxides. NATURE 358, 136–138. doi:{10.1038/358136a0}.

Fornasini, P., Grisenti, R., Dapiaggi, M., Agostini, G., Miyanaga, T., 2017. Nearest-neighbour distribution of distances in crystals from extended x-ray absorption fine structure. The Journal of Chemical Physics 147, 044503. doi:10.1063/1.4995435.

Guguchia, Z., Keller, H., Khler, J., Bussmann-Holder, A., 2012. Magnetic field enhanced structural instability in eutio 3. Journal of Physics: Condensed Matter 24, 492201. doi:10.1088/0953-8984/24/49/492201.

Ikeda, T., Kobayashi, T., Takata, M., Takayama, T., Sakata, M., 1998. Charge density distributions of strontium titanate obtained by the maximum entropy method. Solid State Ionics 108, 151 – 157. doi:https://doi.org/10.1016/S0167-2738(98)00033-2.

Jonane, I., Anspoks, A., Kuzmin, A., 2018. Advanced approach to the local structure reconstruction and theory validation on the example of the w l 3 -edge extended x-ray absorption fine structure of tungsten. Modelling and Simulation in Materials Science and Engineering 26, 025004. URL: http://stacks.iop.org/0965-0393/26/i=2/a=025004, doi:10.1088/1361-651X/aa9bab.

Koehler, J., Dinnebier, R., Bussmann-Holder, A., 2012. Structural instability of EuTiO3 from X-ray powder diffraction. PHASE TRANSITIONS 85, 949–955. doi:{10.1080/01411594.2012.709634}.

Kwei, G.H., Lawson, A.C., Billinge, S.J.L., Cheong, S.W., 1993. Structures of the ferroelectric phases of barium titanate. The Journal of Physical Chemistry 97, 2368–2377. doi:10.1021/j100112a043.

Levin, I., Krayzman, V., Woicik, J.C., Bridges, F., Sterbinsky, G.E., Usher, T.M., Jones, J.L., Torrejon, D., 2016. Local structure in batio$_3$-bisco$_3$ dipole glasses. Phys. Rev. B 93, 104106. doi:10.1103/PhysRevB.93.104106.

Mastelaro, V., Favarim, H., Mesquita, A., Michalowicz, A., Moscovici, J., Eiras, J., 2015. Local structure and hybridization states in ba0.9ca0.1ti1xzrxo3 ceramic compounds: Correlation with a normal or relaxor ferroelectric character. Acta Materialia 84, 164 – 171. doi:https://doi.org/10.1016/j.actamat.2014.10.059.

Miyanaga, T., Diop, D., Ikeda, S.I., Kon, H., 2002. Study of the local structure changes in pbtio 3 by pb l iii exafs. Ferroelectrics 274, 41–53. doi:10.1080/713716404.

Müller, K.A., Burkard, H., 1979. Srtio$_3$: An intrinsic quantum paraelectric below 4 k. Phys. Rev. B 19, 3593–3602. doi:10.1103/PhysRevB.19.3593.

Ravel, B., Newville, M., 2005. Athena, artemis, hephaestus: data analysis for x-ray absorption spectroscopy using ifeffit. Journal of Synchrotron Radiation 12, 537–541. doi:10.1107/S0909049505012719.

Ravel, B., Stern, E.A., Vedrinskii, R.I., Kraizman, V., 1998. Local structure and the phase transitions of batio$_3$. Ferroelectrics 206, 407–430. doi:10.1080/00150199808009173.

Rehr, J.J., Albers, R.C., 2000. Theoretical approaches to x-ray absorption fine structure. Rev. Mod. Phys. 72, 621–654. doi:10.1103/RevModPhys.72.621.

Schiemer, J., Spalek, L.J., Saxena, S.S., Panagopoulos, C., Katsufuji, T., Bussmann-Holder, A., Köhler, J., Carpenter, M.A., 2016. Magnetic field and in situ stress dependence of elastic behavior in eutio$_3$ from resonant ultrasound spectroscopy. Phys. Rev. B 93, 054108. doi:10.1103/PhysRevB.93.054108.

Simonelli, L., Marini, C., Olszewski, W., vila Prez, M., Ramanan, N., Guilera, G., Cuartero, V., Klementiev, K., 2016. Clss: The hard x-ray absorption beamline of the alba cells synchrotron. Cogent Physics 3, 1231987. doi:10.1080/23311940.2016.1231987.

Stern, E.A., 2004. Character of order-disorder and displacive components in barium titanate. Phys. Rev. Lett. 93, 037601. doi:10.1103/PhysRevLett.93.037601.

Stuhlhofer, B., Logvenov, G., Grny, M., Roleder, K., Boris, A., Prpper, D., Kremer, R.K., Khler, J., Bussmann-Holder, A., 2016. New features from transparent thin films of eutio3. Phase Transitions 89, 731–739. doi:10.1080/01411594.2016.1199805.

Timoshenko, J., Anspoks, A., Kalinko, A., Kuzmin, A., 2016. Local structure of copper nitride revealed by exafs spectroscopy and a reverse monte carlo/evolutionary algorithm approach. Physica Scripta 91, 054003. doi:10.1088/0031-8949/91/5/054003.

Timoshenko, J., Kuzmin, A., 2009. Wavelet data analysis of exafs spectra. Computer Physics Communications 180, 920 – 925. doi:https://doi.org/10.1016/j.cpc.2008.12.020.

Timoshenko, J., Kuzmin, A., Purans, J., 2014. Exafs study of hydrogen intercalation into reo 3 using the evolutionary algorithm. Journal of Physics: Condensed Matter 26, 055401. URL: http://stacks.iop.org/0953-8984/26/i=5/a=055401, doi:0.1088/0953-8984/26/5/055401.

Tkacz-Åmiech, K., KoleÅyÅski, A., Ptak, W., 2003. Crystal-chemical aspects of phase transitions in barium titanate. Solid State Communications 127, 557 – 562. doi:https://doi.org/10.1016/S0038-1098(03)00503-9.

Vedrinskii, R.V., Kraizman, V.L., Novakovich, A.A., Demekhin, P.V., Urazhdin, S.V., 1998. Pre-edge fine structure of the 3d atom k x-ray absorption spectra and quantitative atomic structure determinations for ferroelectric perovskite structure crystals. Journal of Physics: Condensed Matter 10, 9561. doi:10.1088/0953-8984/10/42/021.

Institute of Solid State Physics, University of Latvia as the Center of Excellence has received funding from the European Union's Horizon 2020 Framework Programme H2020-WIDESPREAD-01-2016-2017-TeamingPhase2 under grant agreement No. 739508, project CAMART²